atmosphere

MDPI

Article

Analysis of Different Height Correction Models for Tropospheric Delay Grid Products over the Yunnan Mountains

Fangrong Zhou [1], Luohong Li [2,3,*], Yifan Wang [1], Zelin Dai [1], Chenchen Ding [4], Hui Li [5] and Yunbin Yuan [2]

[1] Electric Power Research Institute, Yunnan Power Grid Company Co., Ltd., Kunming 650217, China; zhoufangrong@dlyjy.yn.csg.cn (F.Z.); wangyifan@yn.csg.cn (Y.W.); daizelin@yn.csg.cn (Z.D.)
[2] State Key Laboratory of Geodesy and Earth's Dynamics, Innovation Academy for Precision Measurement Science and Technology, Chinese Academy of Sciences, Wuhan 430077, China; yybgps@apm.ac.cn
[3] University of Chinese Academy of Sciences (UCAS), Beijing 100049, China
[4] Public Meteorological Service Center of China Meteorological Administration, Beijing 100081, China; dingcc@cma.gov.cn
[5] College of Surveying and Geo-Informatics, North China University of Water Resources and Electric Power, Zhengzhou 450046, China; lihui@ncwu.edu.cn
* Correspondence: li.luohong@apm.ac.cn

Abstract: Accurate tropospheric delays are of great importance for both Global Navigation Satellite System (GNSS)-based positioning and precipitable water vapor monitoring. The gridded tropospheric delay products, including zenith hydrostatic delays (ZHD) and zenith wet delays (ZWD), are the most ideal method for accessing accurate tropospheric delays. The vertical adjustment method is critical for implementing the gridded tropospheric products. In this work, we consider the different models used for grid products and assess their performance over Yunnan mountains with complex topography. We summarize the main results as follows: (1) The products can provide accurate ZHD with mean biases of −2.6 mm and mean Standard Deviation (STD) of 1.5 mm while the ZWD results from grid products show a performance with biases of −0.4 mm and STD of 1.3 cm over the Yunnan area. (2) The T_v-based model shows a better performance than the T_0-based model and IGPZWD in rugged areas with large height differences. The grid products can provide hourly ZHD with biases of 3 mm and wet delay with mean biases of within 2 cm and mean STD of below 3 cm in the Yunnan mountains, which exhibit a large height difference of around 1.5 km. (3) The radiosondes results confirm that the T_v-based model has an obvious advantage in calculating ZHD height corrections for differences within 2 km while the T_0-model suffers from a loss in accuracy in the case of large height differences. If the site is located more than 1 km below the reference height, the IGPZWD model can provide a better ZWD with a mean bias of 1.5 cm and a mean STD of 1.7 cm. With vertical reduction models, the grid products can provide accurate ZHD and ZWD in real time, even if in complex area.

Keywords: vertical reduction model; zenith hydrostatic delay (ZHD); zenith wet delay (ZWD); tropospheric grid product

Citation: Zhou, F.; Li, L.; Wang, Y.; Dai, Z.; Ding, C.; Li, H.; Yuan, Y. Analysis of Different Height Correction Models for Tropospheric Delay Grid Products over the Yunnan Mountains. *Atmosphere* **2024**, *15*, 872. https://doi.org/10.3390/atmos15080872

Academic Editors: Sergey Pulinets and Yuichi Otsuka

Received: 24 April 2024
Revised: 4 July 2024
Accepted: 11 July 2024
Published: 23 July 2024

1. Introduction

The troposphere contains three-quarters of the mass of the entire atmosphere, including abundant water vapor. Signals from Global Navigation Satellite Systems (GNSS) are delayed and bent because of interaction with dry gases and water vapor along the propagation path in the troposphere [1]. Tropospheric delay is one of the major error sources and should be carefully addressed in GNSS applications. The external tropospheric corrections can be provided by the tropospheric grid product or other products, which provide an accurate initial value for zenith hydrostatic delay (ZHD), enabling precise estimation of the zenith wet delay (ZWD) in Precise Point Positioning (PPP) [2]. Moreover, modeling ZHD is crucial for GNSS precipitable water vapor (PWV) retrieval [3,4], which is a common technique for water vapor monitoring. However, it is still very challenging to accurately

correct the zenith tropospheric delay in real time due to complex temporal and spatial variations.

As it is difficult to directly measure these delays with sufficient accuracy, the delays are mapped into zenith direction, namely zenith tropospheric delay (ZTD), consisting of ZHD and ZWD. Conventional tropospheric delay models such as the Hopfield model [5] and the Saastamoinen model [6] may achieve centimeter-level accuracy with accurate in-situ meteorological observations. However, most GNSS sites are not equipped with meteorological sensors and there are often no co-located weather stations near GNSS sites. Thus, it is hard to directly use the above empirical models to obtain the accurate ZHD and ZWD. The troposphere delay can also be modeled by time and location based on historical reanalysis products in empirical models without meteorological data as inputs, such as Global Pressure and Temperature (GPT) series models [7,8]. The GPT3 is the latest version of the GPT series models, providing meteorological parameters such as temperature, pressure, water vapor pressure, and lapse rate in temperature at any position on the Earth's surface [9]. It should be noted that the empirical models only simulate the annual and semiannual variations of ZTD but they have obvious limitations when modeling rapid ZTD variations in real-time cases, especially during extreme weather events [10].

Numerical Weather Models (NWM) can provide hourly ZTD with an accuracy of 1–2 cm [11]. Tropospheric delays from a high-resolution NWM model are given on a horizontal grid since the vertical approximation of the tropospheric delay is derived by Dousa and Elias [12] and Wang, et al. [13] from the barometric formula [14] and the model of Askne and Nordius [15]. The implementation of NWM-based troposphere products requires a highly accurate vertical reduction function, which can convert the tropospheric delay at grid height to the station height.

In order to obtain accurate ZHD and ZWD in real time, researchers proposed a ZHD/ZWD model based on the predicted NWM products [16,17]. Such global grid products, including the hydrostatic and wet zenith delays as a by-product of Vienna mapping function 1 (VMF1), are determined from forecasts of the European Centre for Medium-Range Weather Forecasts (ECMWF) based on the ray-tracing techniques [18]. The two grid products based on the latest Vienna mapping function 3 (VMF3) are released with intervals of 6 h using ECMWF operational and forecasting analysis, namely VMF3-OP and VMF3-FC [9]. Yuan, et al. [19] retrieved integrated water vapor from ground-based GPS stations with the above troposphere grid products. Similar to the fifth-generation reanalysis model (ERA5) of ECMWF, the Global Forecast System (GFS) products are produced by the National Centers for Environmental Prediction (NCEP), providing global forecasts of atmospheric variables at 26 isobaric levels on a spatial grid of $0.25^\circ \times 0.25^\circ$. The Numerical Weather Prediction (NWP) model has a significant potential for real-time tropospheric delay corrections [20]. To improve the accessibility and time resolution of ZHD and ZWD in real time, a new forecasting tropospheric product has been proposed based on the NWP forecasts [21]. The ZHD and ZWD are calculated by integration of the forecasted pressure level data of NCEP-GFS and are released by the global grid at an interval of 1 h.

The choice of an appropriate vertical reduction method is important for implementing the above grid products. Zhang, et al. [22] presented a refined method for vertical reduction by implementing VMF3-like ZHD products for the Tibetan plateau and its surroundings, improving 70% in ZHD compared to the conventional method. The results confirmed that the vertical reduction model is very important for the single-level troposphere grid products. Jiang, et al. [23] established a new global pressure and ZWD model with a three-order exponential function, namely IGPZWD, which is used to express the relationship between Pressure/ZWD and height, and its fitted coefficients are modeled as a function of the latitude, longitude, day of the year (DOY) and hours. Li, et al. [24] also optimized vertical reduction functions in ZTD to improve the performance of the IGGtrop model in the Northern Hemisphere. Yao and Hu [25] proposed an HZWD model with built-in piecewise height functions to simulate ZWD vertical variation. There have been many attempts to improve the performance of vertical reduction in ZHD and ZWD, but most

works focus on the tropospheric empirical models instead of the forecasting grid products, which can be used in real-time applications. Moreover, few works pay attention to the improvement of the vertical reduction in ZWD, especially in the case of mountainous areas with significant height differences. The impact of vertical reduction on troposphere grid products should be clear before retrieving the GNSS-PWV or correcting the tropospheric delay in PPP applications. In addition, the measured in situ pressure should be converted from the sensor height to the GNSS site height with vertical reduction models in the GNSS meteorological station. Thus, vertical reduction is an important issue for troposphere-related data processing.

In this research, we focused on the impact of vertical reduction on the implementation of the forecasted tropospheric delay grid product. Different approaches for vertical reduction in ZHD and ZWD are validated based on muti-source data, including in situ pressure, ERA5, and radiosonde profiles. The rest of this article is organized as follows: the datasets and vertical reduction models used in this article are described in the Section 2. The Section 3 part presents the evaluations of the products at grid point height and the performances of vertical reduction for grid products. Different height differences are studied in detail. The conclusions are drawn last.

2. Method and Data

2.1. Data

The GNSS water vapor products are generated by the Meteorological Center of China Meteorological Administration (CMA) for weather diagnoses and forecasting applications and include the measured in situ surface air pressures and temperatures at GNSS sites and GNSS-ZTD. The pressure and temperatures are collected by nearby meteorological sensors. The sampling time interval is 30 min. We collected two months of data from 29 stations located in the Yunnan mountains, where the products in June represent summer time while those in October represent winter time.

The fifth-generation reanalysis model (ERA5) is the latest climate reanalysis model from the European Centre for Medium-Range Weather Forecasts (ECMWF), replacing ERA-Interim. ERA5 takes both physical models and observations into account to describe the state of the atmosphere numerically. The ERA5 layer products with 37 pressure layers are utilized with a horizontal resolution of $0.25^\circ \times 0.25^\circ$ and a temporal resolution of 1 h (https://cds.climate.copernicus.eu). The ZHD and ZWD at grid points height retrieved from ERA5 products are used as reference.

The forecasting tropospheric product is generated based on the numerical weather forecasting products NCEP-GFS, which is developed by [21] and operated routinely in the Innovation Academy for Precision Measurement Science and Technology (APM), Chinese Academy of Science (CAS). The geopotential, temperature, and specific humidity fields from GFS were used to calculate ZHD and ZWD at each $1.0^\circ \times 1.0^\circ$ grid. The grid is released in 1 h intervals and several hours in advance. APM forecasting products are provided via the FTP server.

Data gathered in 2023 from six radiosonde stations located in the Yunnan mountains and surrounding area were used, including Xichang (56571), Weining (56691), Kunming (56778), Mengzi (56985), Simao (56964), and Tengchong (56739). They provide high-resolution vertical profiles of height, temperature, relative humidity, wind speed, and wind direction. The profiles are collected by each station at 0000 and 1200 UTC. Time series of ZHD and ZWD in 2023 at different heights are integrated using the daily profiles of radiosonde stations. These data were downloaded from a radiosonde database of the Department of Atmospheric Science of the University of Wyoming (http://weather.uwyo.edu/upperair/bufrraob.shtml (accessed on 5 March 2024)).

The measured in situ pressure data in 2023 from 33 distributed meteorological stations over Yunnan and its surrounding areas are accessed from the Integrated Surface Database (ISD) of the National Oceanic and Atmospheric Administration (NOAA) of the United States. The time interval of pressure data is 3 h. Most of the stations are in CHINA and are

routinely operated by CMA. The site's longitude, latitude, and height can be obtained from the data files. The distribution of grid points, GNSS stations, meteorological stations, and radiosonde stations used is plotted in Figure 1.

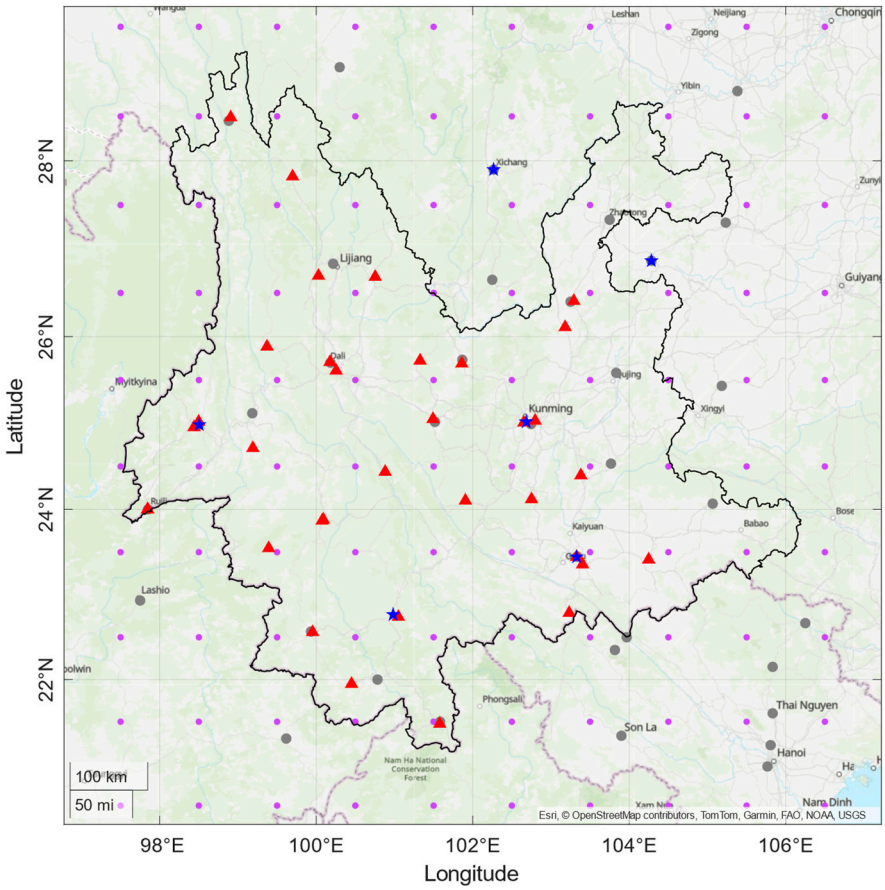

Figure 1. The distribution of grid points (purple dots), GNSS stations (red triangles), meteorological stations (grey dots), and radiosonde (blue pentagram) over Yunnan and the surrounding area.

2.2. The Vertical Reduction Models in ZHD

The height of most stations does not coincide with that of the orography in grid products. Since the ZHD can be determined by the Saastamoinen model [6], the height correction of ZHD can be converted to that of pressure. Thus, the vertical modeling of the atmospheric pressure is a crucial step for implementing ZHD grid products, especially over regions with complex topography. Here, we first review three already known methods for this purpose.

T_0-based model

The formula is derived from the dry-air differential equation [14,26] and reads as follows:

$$P_s = P_0 \left(1 - \frac{\alpha}{T_0} h\right)^{\frac{Mg}{\alpha R}} \quad (1)$$

where P_s and P_0 denote the atmospheric pressure (hPa) at the site and mean sea level (MSL), respectively; h is site height; M is the average molecular mass, which is 0.0289644 kg/mol; g is the gravitational acceleration, which is 9.80665 m/s^2; R is the general gas constant, which is 8.31432 (J/K·mol); α is the lapse rate of temperature, which is 6.5 K/Km; and T_0 is the constant temperature at MSL, which is 289 K.

The model uses the temperature and its lapse rate to convert pressure at MSL to site pressure. By introducing the constant parameters, the simplified version reads as follows:

$$P_s = P_g \times \left(1 - 2.26 \times 10^{-5} \times \left(h_s - h_g\right)\right)^{5.255} \quad (2)$$

where P_g is the pressure at the grid point height, the simplified method has been employed by many previous studies for pressure adjustment in height.

T_v-based model

The exponential formula based on the virtual temperature for the vertical reduction in pressure is used in the GPT2 model and inherited by GPT2w and GPT3, namely the T_v-based model. The GPT2/2w/3 model used 37 levels of ERA-Interim data to fit the global temperature lapse rate grid considering the annual and semiannual cycles [27]. Virtual temperature is a modified temperature that includes the effect of humidity. The formula is presented as follows:

$$P_s = P_g \times e^{-\frac{g \times M}{R \cdot T_v} \times (h_s - h_g)} \quad (3)$$

$$T_v = \left(T_0 + dT \times \left(h_s - h_g\right)\right)(1 + 0.6077 \times Q) \quad (4)$$

where T_v denotes the virtual temperature (K), Q denotes the specific humidity (kg/kg), T_0 and dT is the temperature (K), and its lapse (K) at grid points.

IGPZWD

The improved global pressure and ZWD model developed by [23], namely IGPZWD, is based on the Taylor series expansion of Equation (1) and fits the coefficients from 5-year ERA5 hourly reanalysis data using a three-order exponential function, which considers seasonal and intraday variations. The model can be accessed via https://github.com/LNTUgx/GNSS/tree/main/IGPZWD_model (accessed on 5 March 2024). We extract the vertical correction part for pressure and ZWD and its corresponding coefficient grid from the IGPZWD model, namely the IGPZWD method, in this work. The input parameters are forecasted ZHD or ZWD from grid products and their grid points height, instead of the ZHD or ZWD from the original grid of this model. The method can be expressed as follows:

$$P_s = P_g \cdot e^{\beta_1 \cdot (h_s - h_g) + \beta_2 \cdot (h_s{}^2 - h_g{}^2) + \beta_3 \cdot (h_s{}^3 - h_g{}^3)} \quad (5)$$

where β_1, β_2, and β_3 denote the 1–3 order height scale factors of pressure, P_g refers to pressure at the grid point; P_s is the site pressure, which can be converted to site ZHD with the Saastamoinen model.

2.3. The Vertical Reduction Models in ZWD

Water vapor scale height (WSH) is the key parameter for vertical reduction models in ZWD. The WSH is defined as follows:

$$\rho_h = \rho_0 \cdot e^{-\frac{h}{H}} \quad (6)$$

where ρ_h and ρ_0 denote the water vapor density at height h and that at the surface, respectively; H is water vapor scale height.

Constant WSH model (CWSH)

The commonly used correction method in ZWD takes the WSH as a constant, which can be obtained from the average of the gridded-site differences. The constant WSH used in [28] rewrites as follows:

$$ZWD_s = ZWD_g \cdot e^{-(h_s - h_g)/2000} \quad (7)$$

Due to the varying character of water vapor, the WSH should also be considered a time-varying value. Similar to pressure, the vertical ZWD profiles can also be accurately fitted

using a three-order exponential function in IGPZWD, introducing annual and semi-annual harmonics. The vertical reduction model for ZWD can be expressed as follows:

$$ZWD_s = ZWD_g \cdot e^{\alpha_1 \cdot (h_s - h_g) + \alpha_2 \cdot ({h_s}^2 - {h_g}^2) + \alpha_3 \cdot ({h_s}^3 - {h_g}^3)} \quad (8)$$

where α_1, α_2, and α_3 denote the first-, second-, and third-order height scale factors of ZWD; ZWD_g refers to the ZWD at grid point height; ZWD_s is the site ZWD.

3. Results

In this section, we first assess the overall performance of grid products at grid point height, including ZHD and ZWD. We used the measured in situ pressure in 2023 to assess three vertical reduction models for ZHD and we used the retrieved ZWD from GNSS-ZTD to verify the vertical reduction models for ZWD. The performance of those models for varying height differences cases is validated with the result from radiosonde profiles data as a reference.

3.1. The ZHD and ZWD Performance from Grid Products

We evaluated the overall performance of grid products with respect to ERA5 over the Yunnan mountains. The ZHD and ZWD are determined via vertical integration of ERA5 profiles, referred to as ERA5-ZHD and ERA5-ZWD in the following. The hourly ZHD and ZWD products at 100 grid points in 2023 are computed, covering the region from 20.5° N to 29.5° N in latitude and from 97.5° E to 106.5° E in longitude. The period covers the whole year 2023.

We present the time series of the ZHD and ZWD results from grid products and ERA5 at grid point (26.5° N, 99.5° E, 3118.39 m) to show their different temporal characters in Figure 2. We can see that the ZHD is stable while the ZWD shows a significant seasonal variation reaching its peak in summer. The differences w.r.t ERA5 are larger for ZWD than for ZHD. Rapid variations of ZWD are expected to complicate the maintenance of the quality after vertical adjustment for the height reduction model.

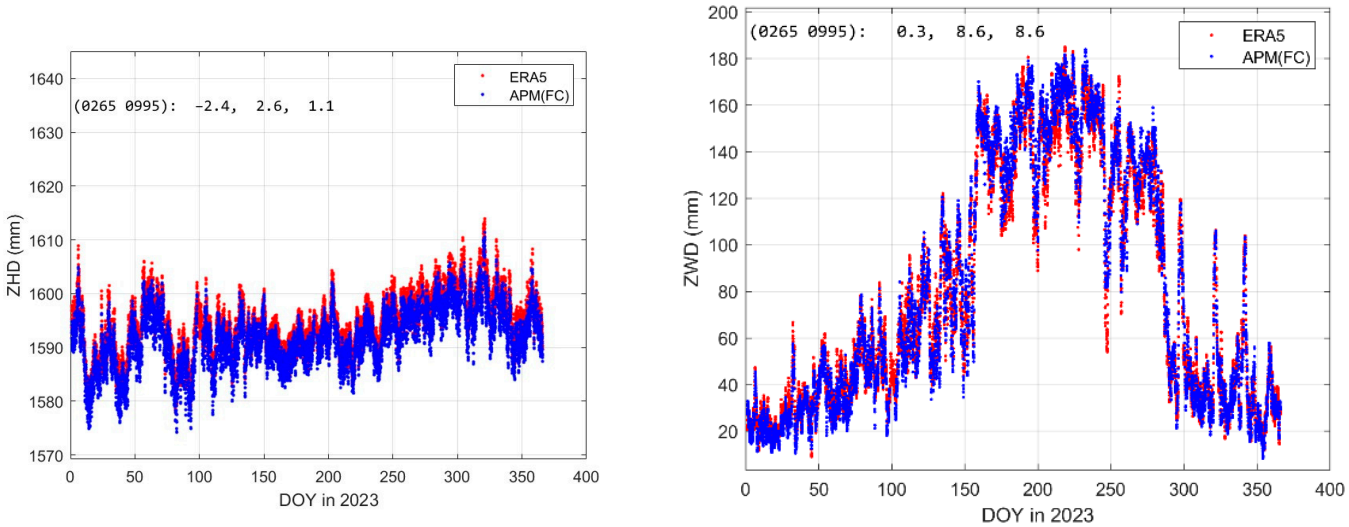

(**a**) (**b**)

Figure 2. The difference in ZHD (**a**) and ZWD (**b**) at grid point (26.5° N, 99.5° E, 3118.39 m) from the grid products compared with ERA5. The text from left to right labeled in the figure is Bias, RMS, and STD, respectively.

The spatial distribution of biases and Standard Deviation (STD) in ZHD from grid products is plotted in Figure 3. The grid products can provide accurate ZHD with biases of 2.6 mm and STD of 1.5 mm over the Yunnan area, which is sufficient for GNSS water

vapor retrieval without meteorological parameters. Due to the character of time variation, the ZWD results from grid products show accuracy with biases of −0.4 mm and an STD of 13.3 mm. The spatial distribution of ZWD biases and STD are shown in Figure 4. In ZWD STD, an obvious trend from south to north can be observed, which is related to the height of grid points in south Yunnan being lower than that in north Yunnan, and the wet delay in grid points in south Yunnan varies more actively than that in the north. However, the grid products can still provide a better alternative for ZWD with around 15 mm in STD, where ZWD values from the traditional method and Machine Learning (ML)-based method have overall root mean square (RMS) errors of 20 mm [29,30].

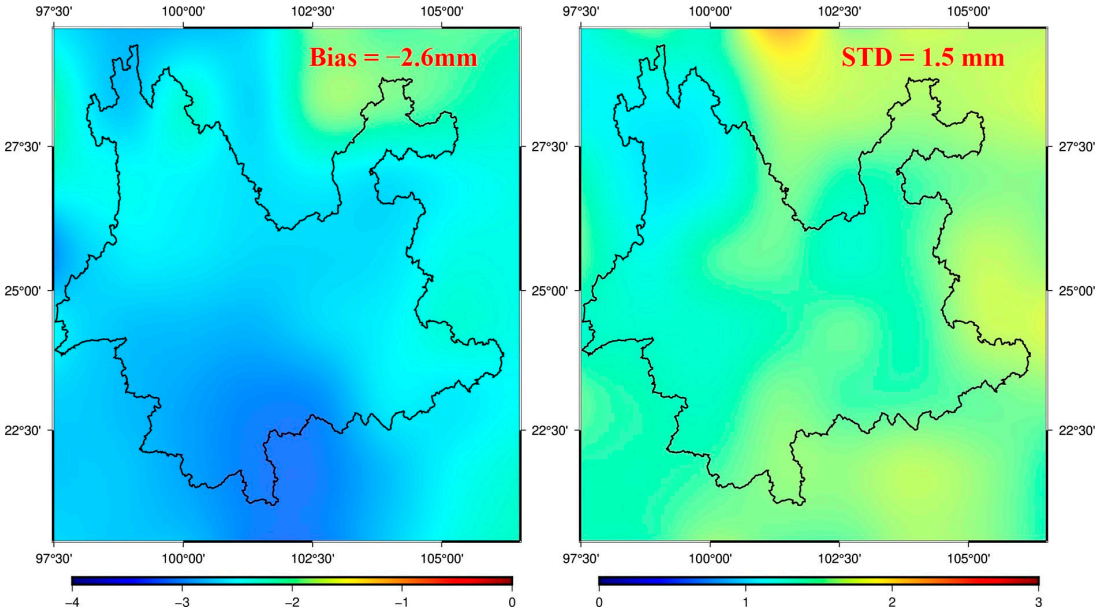

Figure 3. Mean Bias and STD of ZHD derived from grid products with respect to ERA5 over the Yunnan mountains.

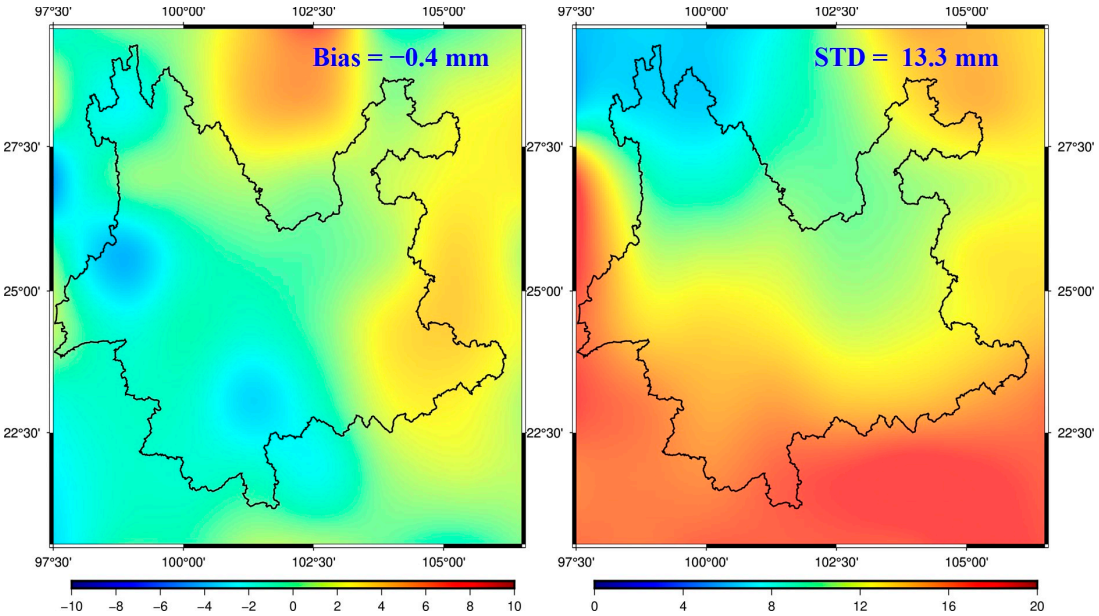

Figure 4. Mean Bias and STD of ZWD derived from products with respect to ERA5 over the Yunnan mountains.

In conclusion, the grid products can provide an hourly ZHD and ZWD over Yunnan in forecasting mode, which shows good performance with respect to ERA5. With the assessment of forecasting tropospheric products, we can implement this product to provide real-time atmospheric information to advance the PPP users and monitor the water vapor, making use of the abundant GNSS stations without the need for meteorological parameters.

3.2. The Vertical Reduction Models Validated by Measured Meteorological Data

The sophisticated vertical reduction model can not only maintain the quality of tropospheric delay after vertical adjustment but can also improve the implementation accuracy of grid products. The vertical reduction model in ZHD should be different from that in ZWD because ZHD is determined by pressure while ZWD is determined by water vapor. Thus, we use the different surface meteorological data to validate the impact of the vertical reduction model in ZHD and ZWD.

As for ZHD, we used the pressure routinely recorded by surface meteorological stations. The Saastamoinen model is used to convert ZHD from pressure. The calculated ZHD is finally used for validating ZHD vertical correction models.

We assess three vertical reduction models based on the surface meteorological data, including IGPZWD, T_0-based model, and T_v-based model. The biases and STD in ZHD of grid products after vertical reduction are calculated and listed in Table 1. To clarify the results, we first calculated the mean bias and mean STD at each station based on the entire time series of ZHD/ZWD differences for each model. Then, we calculated the Min/Mean/Max value in terms of Bias and STD based on the statistical results of all the stations used. The results indicate that the T_v-based model shows a better performance in terms of biases and STD than IGPZWD and the T_0-based model, where those two models are built based on the function of height differences while the temperature is considered in the T_v-based model. The largest bias and STD are found for the T_0-based model, which is constituted in the constant temperature. However, the minimum bias and STD of all three models are very close, which indicates that all three models show a good performance in case of small height differences.

Table 1. The biases and STD in ZHD with three vertical reduction models (mm).

Model	Biases Mean [Min, Max]	STD Mean [Min, Max]
IGPZWD	1.0 [−3.5, 6.1]	2.3 [1.5, 5.9]
T_0-based model	−0.3 [−7.1, 6.7]	2.7 [1.5, 8.0]
T_v-based model	0.4 [−3.0, 5.3]	2.3 [1.4, 4.4]

We also demonstrate the result of implementing the three vertical reduction models for ZHD, using two cases under different height difference scenarios in Figure 5. The above-noted three models show good performance at station 56586 in Figure 5a, reaching a bias within 0.3 mm and an STD of 2.1 mm, where the weighted mean difference between site height and the height of the four near grid points is 28 m. As shown in Figure 5b, the largest height difference was observed in station 48803, reaching 1617 m, where the biases of IGPZWD and T_v-based models at station 48802 are −3.5 mm and −0.6 mm, respectively. The worst STD of around 8 mm is obtained by the T_0-based model while the STD of the IGPZWD and T_v-based models are around 4.9 and 4.4 mm, respectively. We can conclude that the three models can provide a good vertical reduction for grid products over small height difference cases, rapidly decreasing in accuracy in cases of height differences over 800 m. Among the three above-mentioned models, the T_v-based model can maintain the quality of ZHD after vertical reduction, showing a good performance in cases of large height differences.

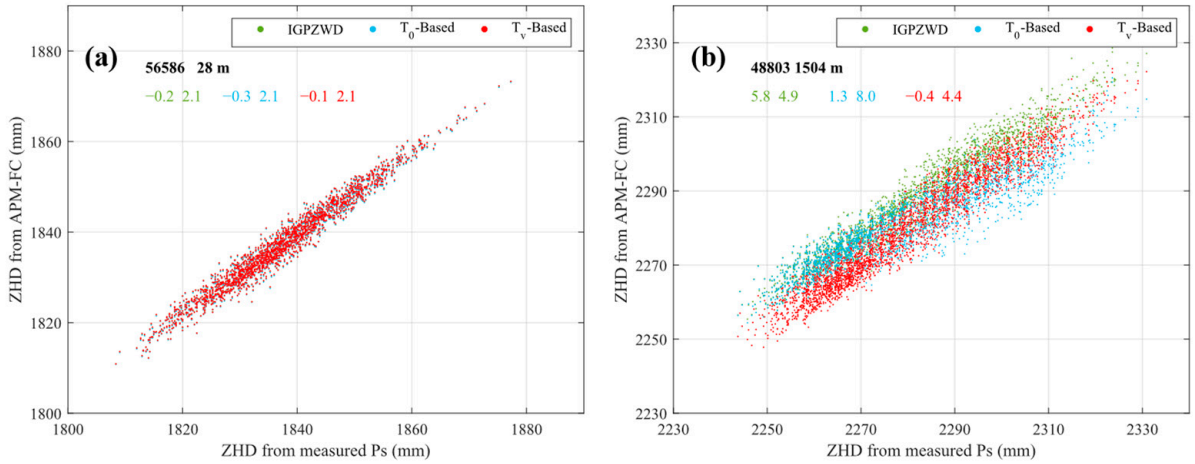

Figure 5. The performances in ZHD (mm) from grid products with IGPZWD, T_0-Based model, and T_v-based model at station 56586 (**a**) and station 48803 (**b**). The text from left to right labeled in the figure is Bias and STD for each model, respectively. The height differences between the site and grid reference height in meters are listed.

It can be concluded that the T_v-based model shows better performance over other models in large height difference cases while the three models can achieve the same performance with biases of 3 mm in small height differences. Meanwhile, verified by surface-measured meteorological data, the results show that the grid products can provide high-accuracy ZHD for ground sites with the aid of vertical reduction models, reaching biases of around 5 mm and STD of below 3 mm. Comparing the result at grid point height, height adjustment does not result in an obvious accuracy loss in ZHD and enables the implementation of ZHD from grid products in complex orography, especially in areas with large altitude differences.

Due to the characteristics of rapid timely variation, the ZWD implementation quality of vertical reduction models is very hard to ensure. Meanwhile, the wet delay is also difficult to measure directly. Since the ZHD can be determined by pressure, the ZWD can be calculated by subtracting ZHD from ZTD. The GNSS-ZWD is used as a reference in validation for vertical reduction models in ZWD. The IGPZWD and CWSH models are assessed, which are common methods for the implementation of ZWD grid products.

We first provide the statistics of ZWD derived from grid products compared to GNSS-ZWD in Table 2. The IGPZWD model shows a better performance than CWSH. As mentioned in the previous part, the IGPZWD model is built by historical reanalysis using the three-order function of height difference and hourly amplitude. In CWSH, we consider the WSH as a constant value of 2000 m, showing significantly worse biases than the IGPZWD method. The worst bias in CWSH is two times over that of IGPZWD. The worst STD of CWSH reaches 3.3 cm while the worst STD of IGPZWD is 2.8 cm. The time-varying parameter and the optimized fitting function of height differences may be of great help for vertical correction for ZWD.

Table 2. Mean biases and STD in ZWD of IGPZWD and Constant WSH (CWSH) models (cm).

Model	Biases Mean [Min, Max]	STD Mean [Min, Max]
IGPZWD	0.4 [−1.4, 1.6]	1.8 [1.2, 2.8]
Constant WSH	0.7 [2.5, 4.3]	1.9 [1.2, 3.3]

To optimize the vertical correction model of grided ZWD in the prediction model, it should be considered that the water vapor scale height of each grid point is synchronously updated and released hourly with ZWD by the forecasting ZWD service. This new model

can be used as a more flexible and accurate approach than IGPZWD, which is more suitable for the time-varying characteristics of wet delay, especially in forecast mode. The time-varying WSH model designed for grided ZWD is further studied and included in grid products.

We also present two cases under different height differences to demonstrate the performance of two models for ZWD in Figure 6. It is notable that the negative height difference indicates that the stations are below the reference GPs of model orography. The height difference at GNSS station KMIN is around −96 m. In this case, the ZWD with the two models shows good consistency with GNSS-ZWD, where the biases are near zero and the STD is around 1.5 cm. As for the TNCH station with a height difference of 671 m, the CWSH shows the worst result in biases and STD while the IGPZWD model achieves −1.4 cm in biases. When compared with the CWSH model, the IGPZWD model improved by around 44% in biases. The above results have demonstrated that IGPZWD can ensure good performance in maintaining the accuracy of ZWD after height adjustment and good quality can be achieved by grid products.

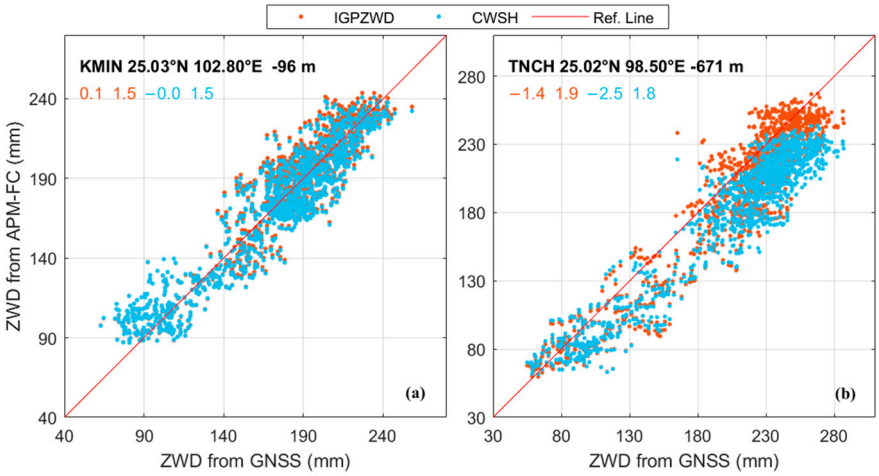

Figure 6. Bias and STD for ZHD with IGPZWD and THCN model implemented at KMIN (**a**) and THCN (**b**). The listed height differences between site and grid reference height are in meters.

Due to the seasonal characteristics in ZWD, we also test the performance at different levels, which can be an important reference for optimizing the vertical reduction models. We take the time series of ZWD differences in June and October with two models at station YNYL as an example in Figure 7. As we know, the wet delay has its peak and largest variations in summer, which makes vertical reduction challenging. We can observe that the CWSH shows a remarkable bias in summer and achieves similar accuracy with IGPZWD in October. As for the IGPZWD model, the bias in summer is 0.9 cm while the bias in autumn is −0.3 cm. The results show that time-varying characteristics should be considered in the vertical reduction model for ZWD and the constant model is not sufficient for this purpose. Because a time-varying character has to be considered, IGPZWD also suffers due to seasonal change but still has a good performance.

The results have confirmed that IGPZWD has a good performance in terms of maintaining an accurate ZWD after height correction for grid products, especially in areas with large height differences. Compared with ZWD accuracy at grid point height, the height correction would cause an accuracy loss due to the complex spatiotemporal changes of ZWD. However, with the help of vertical reduction models, grid products can provide accurate ZWD at one-hour intervals with biases within 2 cm and STD below 3 cm in Yunnan mountains, even for large height differences of around 1.5 km. It is possible for PPP users to introduce ZWD to grid products as an external constraint to advance performance in real-time applications.

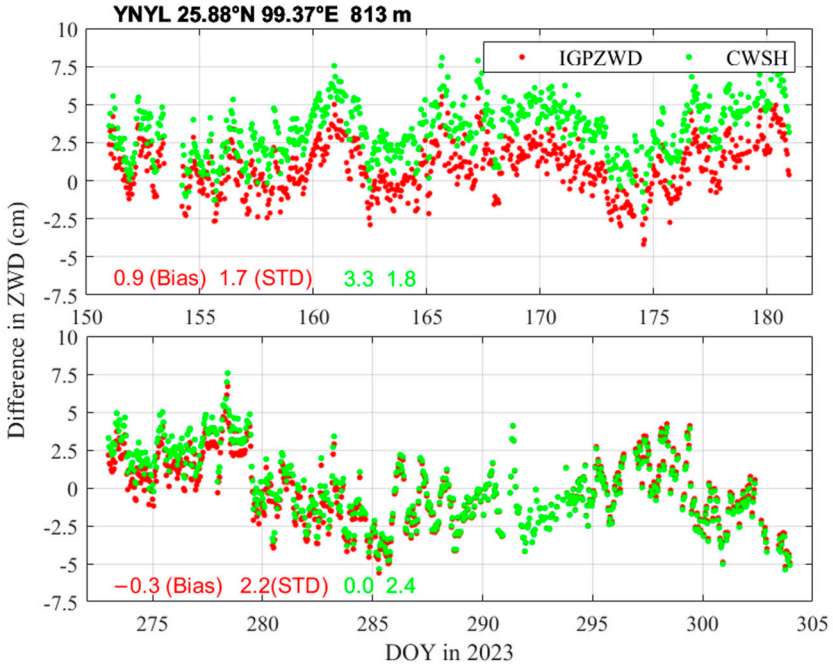

Figure 7. The performances in two vertical reduction models for ZWD (cm) in summer (**upper**) and autumn (**lower**) at station YNYL.

3.3. The Vertical Reduction Models Validated by Radiosondes

To further study the performance of vertical reduction models in ZHD and ZWD at different heights, we use the profile data from six radiosondes in 2023. ZHD and ZWD at different heights are determined via the integration of RS data with the respective height and referred to as RS-ZHD and RS-ZWD. We only conduct the vertical reduction for tropospheric delay with four grid points near radiosondes sites and the ZHD and ZWD at different altitudes with the interval of 0.2 km above/below mean grid point height.

We first showcase the performance of three vertical reduction models for ZHD at RS station 56571 as an example in Figure 8. It can be observed that the T_0-based model suffers from an accuracy reduction due to the large height difference, related to the usage of the fixed lapse rate in temperature (6.5 K/km) and fixed temperature constant (289 K) in this model. However, the temperature and its lapse rates should not be considered constants, if larger temporal and spatial differences exist. The T_v-based model relies on the three-order function of height differences, where the temporary spatial character of the vertical gradient of pressure is modeled by time-varying function coefficients, achieving a better performance than the T_0-based model. Moreover, the T_v-based model shows an obvious advantage in the case of large height differences. Of course, T_v-based corrections will cause accuracy loss due to inaccuracy in the estimated temperature in formula 4 when the height difference exceeds around 3 km while the IGPZWD model has a better performance in case the height difference is larger than 2.5 km.

We also confirm that ZHD from grid products with different vertical reduction models can achieve an RMS of around 8 mm, which is sufficient to aid the GNSS PWV retrieval for stations without meteorological parameters. It should be noted that the T_0-based model has an obvious accuracy loss in cases with large height differences. The biases in ZHD using the T_0-based model increase with height difference.

As for ZWD vertical reduction, we also present the performance of the IGPZWD and CWSH models at six radiosondes stations in Figure 9. The same phenomenon is observed at those stations, where the IGPZWD model performs slightly better than the CWSH model. The water vapor influence on the wet delay is smaller at higher altitudes, as its amount decreases exponentially with height. Therefore, the differences between correction models vanish as the height difference exceeds 2 km. But when we use the models for a case where

the sites are below grid point height, especially near surfaces with higher amounts of water vapor, the two models show an obvious difference. The result in Figure 6 also confirms this point. IGPZWD has a remarkable advantage when compared to the CWSH model.

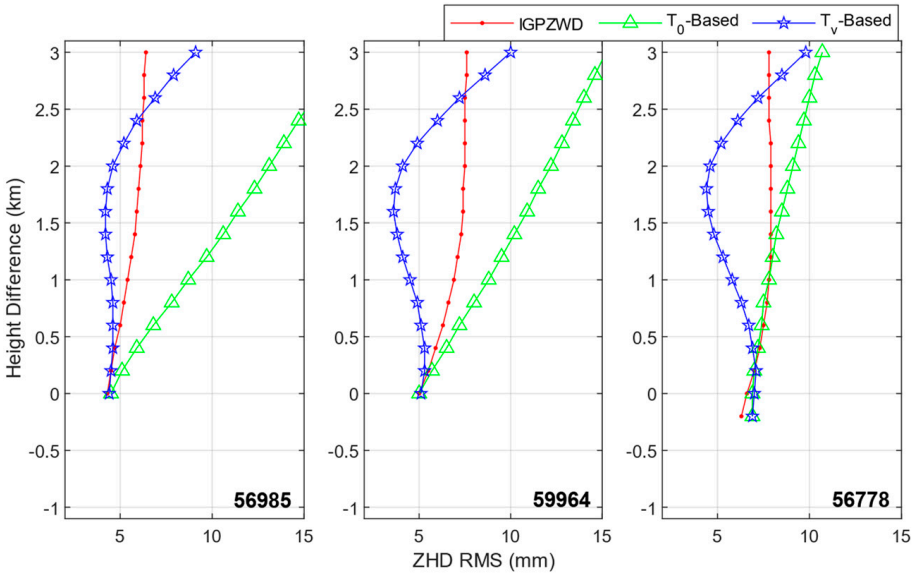

Figure 8. The performance of three vertical reduction models for ZHD (mm) at different height differences at radiosondes station 56778 (25.0° N, 102.3° E), 56964 (22.8° N, 101.0° E), and 56985 (23.4° N, 103.3° E). The zero height refers to the average height of four grid points near the RS sites. The bold text labeled in the figure is the Station Number.

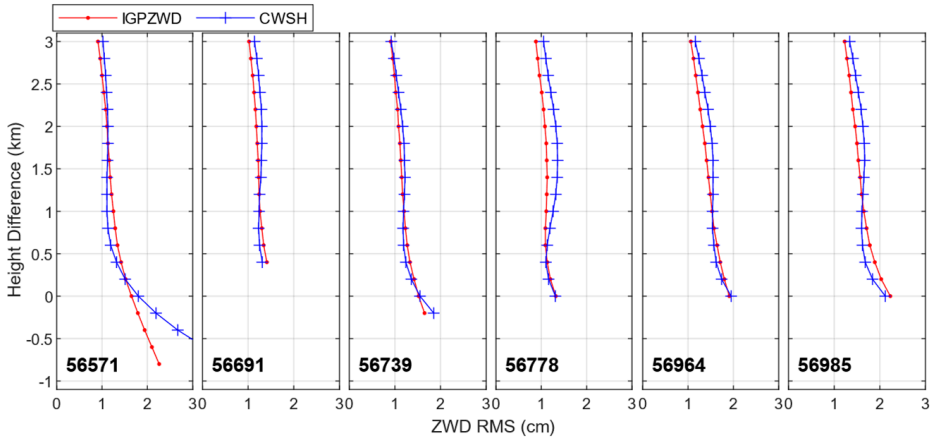

Figure 9. The performance of IGPZWD and CWSH models for ZWD (cm) vertical reduction at different height differences at six radiosondes stations. The zero height refers to the average height of four grid points near the radiosondes sites. The bold text labeled in the figure is the Station Number.

In Figure 10, we show the performance of two vertical reduction models at three altitudes to demonstrate that the accuracy loss is increased as the site height is decreased. We can observe that ZWD has a remarkable difference at three altitudes, where the mean wet delay below 0.6 km from reference height is over 1.7 times that above 0.6 km from reference height, which causes difficulty in vertical reduction. The IGPZWD model is better than the CWSH model at a height lower than the reference height while the IGPZWD model is slightly worse than the CWSH model when we are calculating wet delay at the higher position. Moreover, a seasonal difference in the models' accuracy is also observed, which is related to the ZWD seasonal variation.

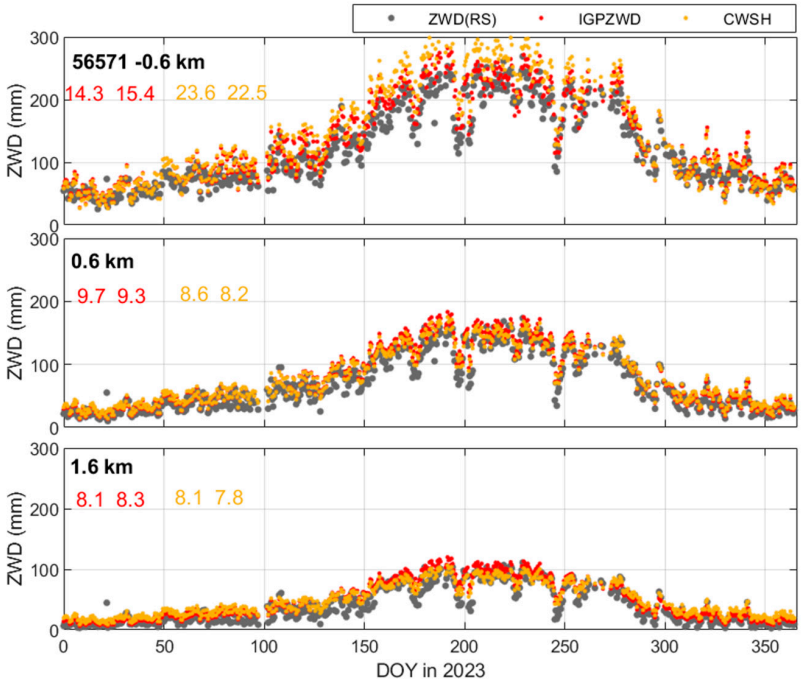

Figure 10. The ZWD (mm) of IGPZWD, CWSH models, and RS-ZWD with different height differences at radiosondes station 56571. The text from left to right labeled in the figure is Bias and STD for each model, respectively. The height differences between the site and grid reference height in meters are listed.

To consider the performance under different ZWD levels, we plot the relationship between the retrieved ZWD error with two models and the referenced RS-ZWD using the time series of ZWD at the height difference of −0.6 km. The retrieved ZWD errors are calculated using the retrieved ZWD after the implementation of two models minus the referenced ZWD. In Figure 11, we found that an equivalent performance was achieved by IGPZWD and CWSH when ZWD is smaller than 120 mm and IGPZWD shows a better performance than CWSH when the RS-ZWD exceeds 120 mm. The IGPZWD model is more accurate and efficient in terms of vertical reduction for ZWD.

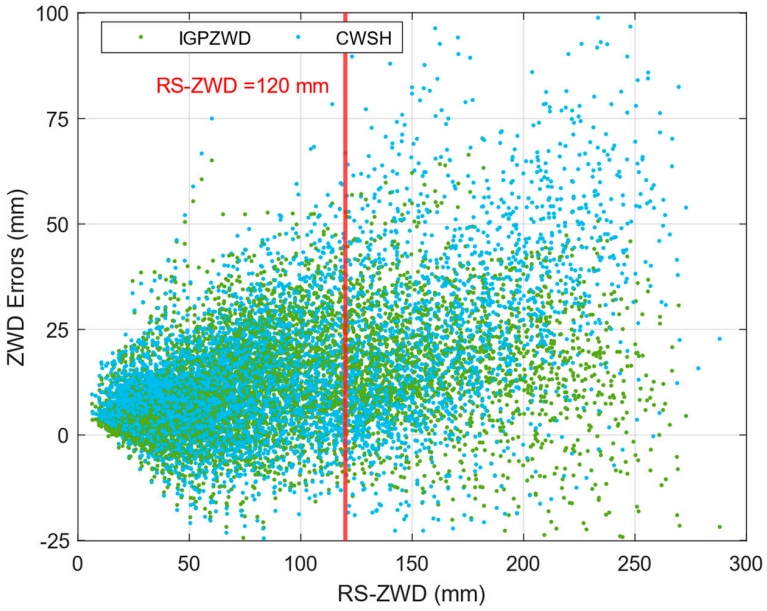

Figure 11. The ZWD errors (mm) after vertical adjustment with the IGPZWD and CWSH models at radiosondes station 56571. The RS-ZWD is used as the reference.

As for the quality of ZWD after height correction, we confirm that the grid products can provide biases of around 0.8 cm and an STD within 1.5 cm when the positive height difference is smaller than 2 km. As the site height is below the reference height and the negative difference is larger than −1 km, the IGPZWD model can provide a better result with around 1.5 cm in biases and 1.7 cm in STD. The ZWD with height correction can provide a good approximate value in PPP applications.

4. Conclusions

High-accuracy vertical correction models are a precondition for the implementation of tropospheric grid products. In this contribution, we study the impact of height correction models on gridded tropospheric delay, in the form of forecasted grids of ZHD and ZWD. First, we analyzed the overall performance of ZHD and ZWD from grid products at grid points' height over the Yunnan mountains, where large height differences exist. Second, the three vertical reduction models for hydrostatic delay and two models for wet delay were assessed with measured in situ pressure and retrieved ZWD from GNSS-ZTD, which lift the tropospheric delay at grid height to site height. Third, we used radiosonde profiles to validate the performance of vertical reduction models at different altitudes. Based on the above results, the following main conclusions are reached:

(1) With respect to ERA5, the grid products can provide accurate ZHD with biases of −2.6 mm and STD of 1.5 mm while the ZWD results from grid products show a performance with biases of −0.4 mm and STD of 1.3 cm over the Yunnan area. It can be concluded that the grid products can provide an hourly accurate ZHD and ZWD over Yunnan in forecasting mode, showing a good performance when compared to ERA5.

(2) Since good quality in ZHD and ZWD can be achieved at grid point height, the vertical reduction model is a key step to implementing grid products. The T_v-based model shows a better performance than the T_0-based model and IGPZWD in large height difference cases, while the models can achieve the same performance in ZHD with biases of 3 mm in small height differences. Compared to the CWSH model, IGPZWD has an improved performance in terms of biases for ZWD with similar STD. The grid products can provide wet delay at one-hour intervals with biases within 2 cm and STD below 3 cm in Yunnan mountains.

(3) A comparison with radiosonde data confirms that the T_v-based model has obvious advantages for height correction in ZHD at large height differences within 2 km while the T_0-based model suffers from accuracy loss due to a big height difference. IGPZWD shows a better performance in case the height difference is larger than 2.5 km. The vertical reduction models for ZWD have similar performances for positive height differences while IGPZWD has a remarkable advantage when compared to the CWSH model at negative height differences. We found that an equivalent performance was achieved by IGPZWD and CWSH when ZWD is lower than 120 mm and IGPZWD shows a better performance than CWSH when the RS-ZWD exceeds 120 mm. As the site height is below the reference height and the negative difference is larger than −1 km, IGPZWD can provide a better result with around 1.5 cm in biases and 1.7 cm in STD.

With the aid of vertical reduction, grid products can provide accurate ZHD and ZWD for ground users, where hourly ZHD with biases of below 3 mm and STD of below 3 mm and ZWD of within 2 cm and STD of below 3 cm are accessed. The ZHD can be of great help for GNSS-PWV retrieval in real-time mode. For PPP users, introducing grid products to ZWD as an external constraint could enhance their performance in real-time applications.

Author Contributions: Author Contributions: Conceptualization, writing—original draft preparation, writing—review and editing, F.Z. and L.L.; methodology and validation, F.Z., L.L. and Y.W.; data curation, Y.W. and L.L.; formal analysis, Z.D., C.D. and H.L.; funding acquisition, Y.W. and Y.Y. All authors have read and agreed to the published version of the manuscript.

Funding: This research was funded by the Science and Technology project of China Southern Power Grid Yunnan Power Grid Co., Ltd. (grant number. YNKJXM20220033).

Institutional Review Board Statement: Not applicable.

Informed Consent Statement: Not applicable.

Data Availability Statement: The reanalysis data provided by the European Centre for Medium Range Weather Forecasts (ECMWF) are available at https://cds.climate.copernicus.eu. The IGPZWD model can be accessed at https://github.com/LNTUgx/GNSS/tree/main/IGPZWD_model (accessed on 5 March 2024). These radiosonde data were downloaded from the Department of Atmospheric Science of the University of Wyoming (http://weather.uwyo.edu/upperair/bufrraob.shtml) (accessed on 5 March 2024). The T_v-based code and grid products are extracted from the GPT3 model, which can be accessed at https://vmf.geo.tuwien.ac.at/codes/ (accessed on 5 March 2024). The pressure data from 30 distributed meteorological stations over Yunan and the sounding area is accessed in the Integrated Surface Database (ISD) at https://www.ncei.noaa.gov/products/land-based-station/integrated-surface-database (accessed on 5 March 2024).

Acknowledgments: We acknowledge the use of Generic Mapping Tools. We also acknowledge the four anonymous reviewers for their insightful insights. We also thank Matthias Aichinger-Rosenberger for helping us improve and polish the text and check the language grammar.

Conflicts of Interest: Authors Fangrong Zhou, Yifan Wang and Zelin Dai were employed by the Yunnan Power Grid Company Co., Ltd. The remaining authors declare that the research was conducted in the absence of any commercial or financial relationships that could be construed as a potential conflict of interest.

References

1. Böhm, J.; Schuh, H. *Atmospheric Effects in Space Geodesy*; Springer: Berlin/Heidelberg, Germany, 2013; Volume 5.
2. Lu, C.; Zhong, Y.; Wu, Z.; Zheng, Y.; Wang, Q. A tropospheric delay model to integrate ERA5 and GNSS reference network for mountainous areas: Application to precise point positioning. *GPS Solut.* **2023**, *27*, 81. [CrossRef]
3. Bevis, M.; Businger, S.; Herring, T.A.; Rocken, C.; Anthes, R.A.; Ware, R.H. GPS meteorology: Remote sensing of atmospheric water vapor using the global positioning system. *J. Geophys. Res. Atmos.* **1992**, *97*, 15787–15801. [CrossRef]
4. Davis, J.; Herring, T.; Shapiro, I.; Rogers, A.; Elgered, G. Geodesy by radio interferometry: Effects of atmospheric modeling errors on estimates of baseline length. *Radio Sci.* **1985**, *20*, 1593–1607. [CrossRef]
5. Hopfield, H.S. Tropospheric effect on electromagnetically measured range: Prediction from surface weather data. *Radio Sci.* **1971**, *6*, 357–367. [CrossRef]
6. Saastamoinen, J. Atmospheric correction for the troposphere and stratosphere in radio ranging of satellites. In Proceedings of the 3rd International Symposium on the Use of Artificial Satellites for Geodesy, Washington, DC, USA, 15–17 April 1971; pp. 247–251.
7. Böhm, J.; Möller, G.; Schindelegger, M.; Pain, G.; Weber, R. Development of an improved empirical model for slant delays in the troposphere (GPT2w). *GPS Solut.* **2015**, *19*, 433–441. [CrossRef]
8. Lagler, K.; Schindelegger, M.; Böhm, J.; Krásná, H.; Nilsson, T. GPT2: Empirical slant delay model for radio space geodetic techniques. *Geophys. Res. Lett.* **2013**, *40*, 1069–1073. [CrossRef]
9. Landskron, D.; Böhm, J. VMF3/GPT3: Refined discrete and empirical troposphere mapping functions. *J. Geod.* **2018**, *92*, 349–360. [CrossRef]
10. Zhang, H.; Yuan, Y.; Li, W. Real-time wide-area precise tropospheric corrections (WAPTCs) jointly using GNSS and NWP forecasts for China. *J. Geod.* **2022**, *96*, 44. [CrossRef]
11. Zhou, Y.Z.; Lou, Y.D.; Zhang, W.X.; Kuang, C.L.; Liu, W.X.; Bai, J.N. Improved performance of ERA5 in global tropospheric delay retrieval. *J. Geod.* **2020**, *94*, 103. [CrossRef]
12. Dousa, J.; Elias, M. An improved model for calculating tropospheric wet delay. *Geophys. Res. Lett.* **2014**, *41*, 4389–4397. [CrossRef]
13. Wang, J.; Balidakis, K.; Zus, F.; Chang, X.; Ge, M.; Heinkelmann, R.; Schuh, H. Improving the Vertical Modeling of Tropospheric Delay. *Geophys. Res. Lett.* **2022**, *49*, e2021GL096732. [CrossRef]
14. Berberan-Santos, M.N.; Bodunov, E.N.; Pogliani, L. On the barometric formula. *Am. J. Phys.* **1997**, *65*, 404–412. [CrossRef]
15. Askne, J.; Nordius, H. Estimation of tropospheric delay for microwaves from surface weather data. *Radio Sci.* **1987**, *22*, 379–386. [CrossRef]
16. Hobiger, T.; Ichikawa, R.; Koyama, Y.; Kondo, T. Fast and accurate ray-tracing algorithms for real-time space geodetic applications using numerical weather models. *J. Geophys. Res. Atmos.* **2008**, *113*, D20302. [CrossRef]
17. Böhm, J.; Schuh, H. Forecasting Data of the Troposphere Used for IVS Intensive Sessions. In Proceedings of the 18th EVGA Working Meeting & 8th IVS Analysis Workshop, 2nd IVS VLBI2010 Working Meeting, Vienna, Austria, 12–15 April 2007.
18. Böhm, J.; Kouba, J.; Schuh, H. Forecast Vienna Mapping Functions 1 for real-time analysis of space geodetic observations. *J. Geod.* **2009**, *83*, 397–401. [CrossRef]
19. Yuan, P.; Blewitt, G.; Kreemer, C.; Hammond, W.C.; Argus, D.; Yin, X.; Van Malderen, R.; Mayer, M.; Jiang, W.; Awange, J.; et al. An enhanced integrated water vapour dataset from more than 10,000 global ground-based GPS stations in 2020. *Earth Syst. Sci. Data Discuss.* **2022**, *15*, 723–743. [CrossRef]

20. Chen, B.; Yu, W.; Wang, W.; Zhang, Z.; Dai, W. A global assessment of precipitable water vapor derived from GNSS zenith tropospheric delays with ERA5, NCEP FNL, and NCEP GFS products. *Earth Space Sci.* **2021**, *8*, e2021EA001796. [CrossRef]
21. Zhang, H. *Study on BDS/GNSS Tropspheric Modeling under Complex Conditions*; The Innovation Academy for Precision Measurement Science and Technology (APM), Chinese Academy of Sciences (CAS): Wuhan, China, 2022.
22. Zhang, H.; Yuan, Y.; Li, W.; Ji, D.; Lv, M. Implementation of Ready-Made Hydrostatic Delay Products for Timely GPS Precipitable Water Vapor Retrieval Over Complex Topography: A Case Study in the Tibetan Plateau. *IEEE J. Sel. Top. Appl. Earth Obs. Remote Sens.* **2021**, *14*, 9462–9474. [CrossRef]
23. Jiang, C.; Gao, X.; Zhu, H.; Wang, S.; Liu, S.; Chen, S.; Liu, G. An improved global pressure and ZWD model with optimized vertical correction considering the spatial-temporal variability of multiple height scale factors. *EGUsphere* **2024**, *2024*, 1–25.
24. Li, W.; Yuan, Y.; Ou, J.; He, Y. IGGtrop_SH and IGGtrop_rH: Two improved empirical tropospheric delay models based on vertical reduction functions. *IEEE Trans. Geosci. Remote Sens.* **2018**, *56*, 5276–5288. [CrossRef]
25. Yao, Y.; Hu, Y. An empirical zenith wet delay correction model using piecewise height functions. In *Annales Geophysicae*; Copernicus Publications: Göttingen, Germany, 2018; pp. 1507–1519.
26. Kleijer, F. Troposphere Modeling and Filtering for Precise GPS Leveling. Ph.D. Thesis, TU Delft Faculty of Aerospace Engineering, Delft, The Netherlands, 2004.
27. Li, T.; Wang, L.; Chen, R.; Fu, W.; Xu, B.; Jiang, P.; Liu, J.; Zhou, H.; Han, Y. Refining the empirical global pressure and temperature model with the ERA5 reanalysis and radiosonde data. *J. Geod.* **2021**, *95*, 31. [CrossRef]
28. Kouba, J. Implementation and testing of the gridded Vienna Mapping Function 1 (VMF1). *J. Geod.* **2008**, *82*, 193–205. [CrossRef]
29. Li, Q.; Yuan, L.; Jiang, Z. Modeling tropospheric zenith wet delays in the Chinese mainland based on machine learning. *Gps Solut.* **2023**, *27*, 171. [CrossRef]
30. Li, Q.; Böhm, J.; Yuan, L.; Weber, R. Global zenith wet delay modeling with surface meteorological data and machine learning. *GPS Solut.* **2024**, *28*, 57. [CrossRef]